THE GEOLOGICAL SOCIETY OF AMERICA®

Evidence of widespread wildfires in a coal seam from the middle Permian of the North China Basin

Yuzhuang Sun[1,*], Cunliang Zhao[1], Wilhelm Püttmann[2], Wolfgang Kalkreuth[3], and Shenjun Qin[4]

[1]KEY LABORATORY OF RESOURCE EXPLORATION RESEARCH OF HEBEI, HEBEI UNIVERSITY OF ENGINEERING, HANDAN 056038, HEBEI, CHINA
[2]INSTITUTE OF ATMOSPHERIC AND ENVIRONMENTAL SCIENCES, GOETHE-UNIVERSITY FRANKFURT AM MAIN, ALTENHÖFERALLEE 1, D-60438 FRANKFURT AM MAIN, GERMANY
[3]INSTITUTO DE GEOCIÊNCIAS, UNIVERSIDADE FEDERAL DO RIO GRANDE DO SUL, AVENIDA BENITO GONÇALVES, 9500, 91501-970 PORTO ALEGRE, RIO GRANDE DO SUL, BRAZIL
[4]HEBEI COLLABORATIVE INNOVATION CENTER OF COAL EXPLOITATION, HEBEI UNIVERSITY OF ENGINEERING, HANDAN 056038, HEBEI, CHINA

ABSTRACT

The North China Basin is the largest coal-bearing basin in China, and has an areal extent of 800,000 km^2. We analyzed 138 coal samples and in situ pillar coal samples of the middle Permian from this basin by macropetrography, microscope, scanning electron microscope, gas chromatography, and gas chromatography–mass spectrometer in order to study wildfires. High contents of inertinite (charcoal) and natural coke particles observed in coal samples indicate that vegetation in precursor mires and peats of the middle Permian coal from north China was exposed to far-ranging wildfires. In addition, high-molecular-weight polycyclic aromatic hydrocarbons were detected in the coal samples. These aromatic compounds were formed under high temperatures and provide further evidence of wildfire. These wildfires would have discharged significant CO and CO_2 gases into the atmosphere and affected the paleoclimate and paleoecosystem.

LITHOSPHERE doi:10.1130/L638.1

INTRODUCTION

The influence of wildfires in the Earth system gained importance after the first plants occupied continental environments (during the Ordovician–Silurian), consuming O_2, raising CO and CO_2, and increasing atmospheric temperature, thus affecting vegetation and changing the climate (Belcher et al., 2013; Lenton, 2013; Rimmer et al., 2015; Scott et al., 2016). Wildfire frequency is currently increasing and the interrelationships between wildfire and mankind are the subject of expanding scientific research (Scott et al., 2016). The study of paleowildfires during Earth evolution can be meaningful for projections of future climate changes (Flannigan et al., 2009).

The role of wildfires at the Permian-Triassic boundary (PTB) has been investigated by many (e.g., Thomas et al., 2004; Xie et al., 2007; Grasby et al., 2011; Shen et al., 2011; Abu Hamad et al., 2012). Shen et al. (2011) studied widespread wildfires close to the PTB, and believed that wildfire, along with fire-derived products, could have contributed to the PTB mass extinction. Widespread wildfires during the Permian Period were also identified in the southern continent of Gondwana (Singh and Shukla, 2004; Jasper et al., 2011, 2013, 2016a, 2016b; Manfroi et al., 2015; Kauffmann et al., 2016). Singh and Shukla (2004) reported that inertinite contents reached 23%–59% of Gondwana coals as a result of wildfires. Jasper et al. (2013) investigated the paleowildfires through a paleobotanical approach. Manfroi et al. (2015) and Kauffmann et al. (2016) found evidence of wildfires in the Brazilian middle and late Permian, respectively. Uhl and Kerp (2003), Noll et al. (2003), and Uhl et al. (2004, 2008, 2012) reported wildfires in the late Paleozoic of central Europe. Wang and Chen (2001) found evidence of paleowildfires through fossils in the sandstones of the uppermost Permian section in north China. Yan et al. (2016) found charcoal layers evidencing wildfires within a coal bed from the early Permian in north China.

The Carboniferous-Permian transition occurred during an overall drying trend in the climate during the final stages of the formation of the megacontinent Pangea (DiMichele et al., 2009). However, many believe that the north China microcontinent was surrounded by tropical oceans during the Carboniferous-Permian transition, and that the climate was wet and tropical (DiMichele et al., 2009; Wang and Pfefferkorn, 2013). High concentrations of inertinite have been found at one section of Dongpang coal mine in the middle Permian coal from the North China Basin by Sun et al. (2002); however, they did not recognize widespread wildfire and its significance. Furthermore, three floral extinction events in north China in the upper middle Permian Period (the Xiashihezi Formation; formerly the Low Shihhotse Formation) were reported by Stevens et al. (2011).

The purpose of this paper is to study the distribution of wildfire under wet tropical climate conditions and its occurrence and scale throughout the North China Basin, and the relevance of the three floral extinction events in the basin.

GEOLOGICAL SETTING

The North China Basin developed on the North China craton (Dai et al., 2008a) and occurs in the northern part of the Sino-Korean craton (Zhao et al., 2006). It is surrounded by the Central Asian orogenic belt and Qinling-Dabie and Sulu orogens (Fig. 1) (Li, 2006). Basement rock of the basin includes Archean rocks with Proterozoic sedimentary cover (Wan and Zeng, 2002). The oldest preorogeny strata are Cambrian. The Cambrian rocks consist of marine sediments, including gray quartz sandstone, dolomite, shale, limestone, and marl. Seawater covered the entire basin

Yuzhuang Sun http://orcid.org/0000-0001-5462-3965
*Corresponding author. sun_yz@hotmail.com

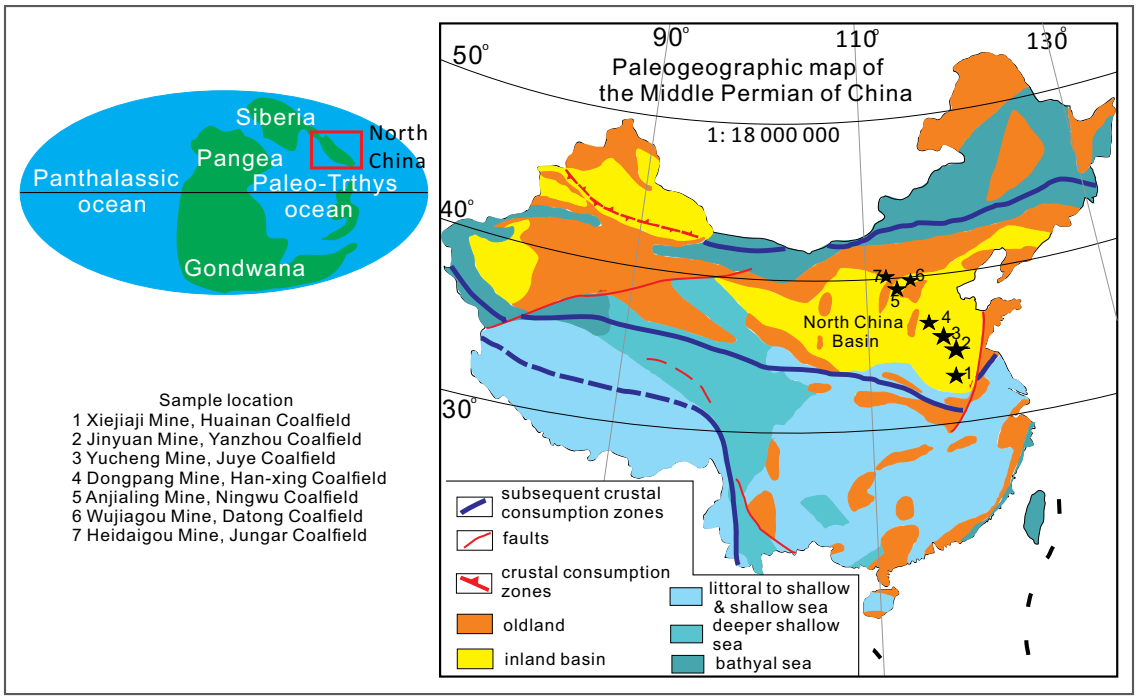

Figure 1. Paleogeographic map of the middle Permian Period in China (modified from Wang et al.,1985).

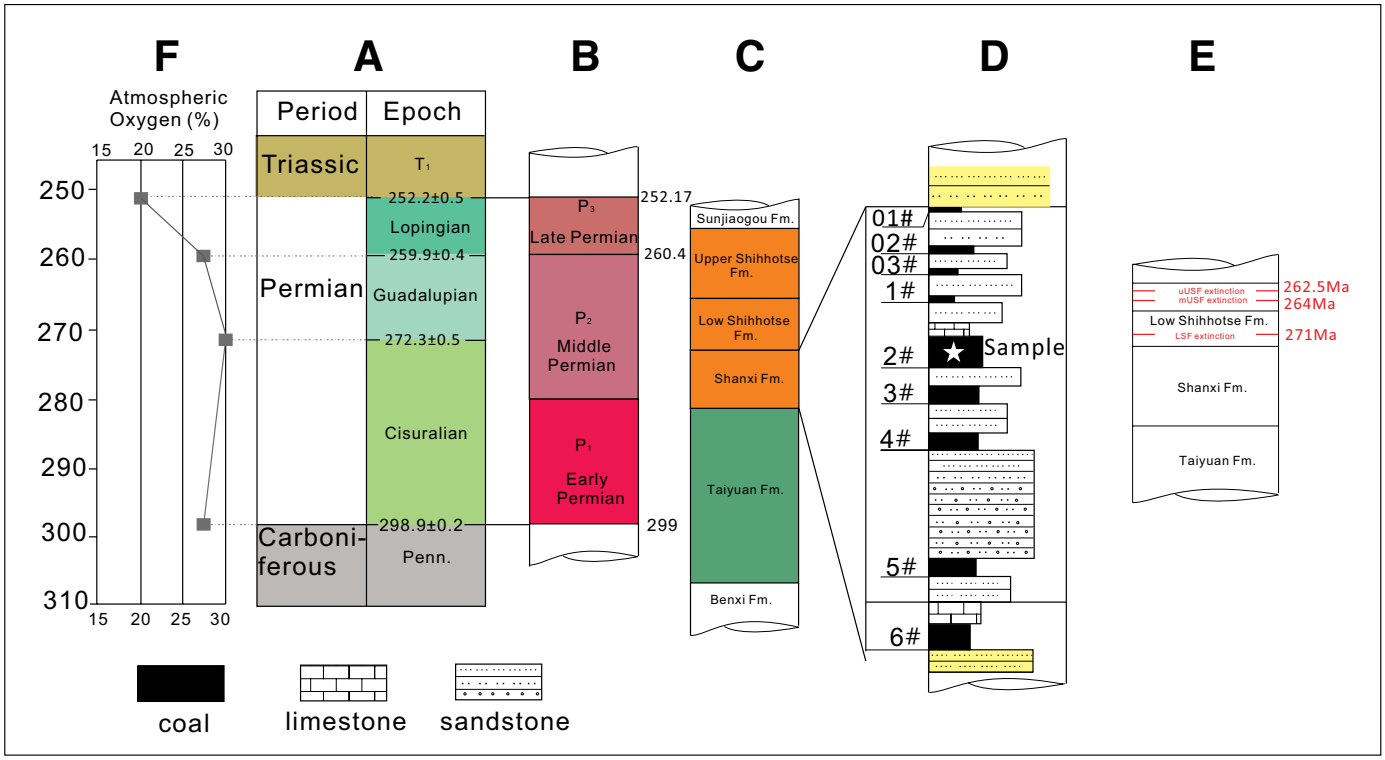

Figure 2. Stratigraphic section of the Permian Period in the North China Basin (modified after National Committee of Stratigraphy of China, 2014). In the Chinese geologic time scale, the Guadalupian-Lopingian boundary (middle-late Permian boundary) has been confirmed with a date of 260.1 Ma. The middle-early Permian boundary has not been confirmed (National Committee of Stratigraphy of China, 2014). (A) Worldwide geologic time scale (Walker and Geissman, 2009). Penn.—Pennsylvanian. (B) Geologic time scale of China (National Committee of Stratigraphy of China, 2014). (C) Stratigraphic chart of North China Basin (National Committee of Stratigraphy of China, 2014) (Fm.—formation). (D) Coal bearing strata of North China Basin. (E) Time of three floral extinctions (modified from Stevens et al., 2011). (F) Variation of atmospheric oxygen level in the geological period studied (modified from Berner, 2006; Scott and Glasspool, 2006).

during the Cambrian Period. The Early to Middle Ordovician rocks consist of epicontinental carbonate sediments. After the Middle Ordovician Period, the Sino-Korean craton was uplifted and subjected to substantial erosion. Sediments of the Silurian, Devonian, and part of the early Carboniferous are absent in the North China Basin because of the uplift of the North China craton during the late-early Paleozoic (Li et al., 2010). This uplift was followed by a period of subsidence that resulted in a major transgression event from the northeast during the middle Carboniferous Period when the craton once again was covered by an epicontinental sea. In the Permian, sandstone, siltstone, oil shale, clay, and coal-forming plants were deposited in delta, river, and lagoon environments. The coal-bearing Taiyuan Formation (upper Pennsylvanian–lower Permian) and the Shanxi Formation (middle Permian) was formed subsequently (Han and Yang 1980) (Figs. 2A, 2B). The sediments from the Permian Shanxi Formation were deposited in a fluvial-dominated deltaic depositional environment (Han and Yang, 1980). A megacoalfield (800,000 km^2) formed during the Carboniferous–Permian Periods in the North China Basin. The middle Permian Shanxi Formation has three to seven coal seams (Figs. 2C, 2D). Approximately 5400 Gt of coals existed in the middle Permian Shanxi Formation (coal density 1.5 T/m^3). In this study, all samples were taken from the No. 2 seam (a primary seam with a thickness of 2–16 m, average 4.5 m) in the middle part of the Shanxi Formation (Fig. 2D).

SAMPLING AND METHODS

Sampling

Coal samples were collected from the inner side of fresh mining faces (Fig. 3A). A total of 138 channel samples of the No. 2 coal seam of the middle Shanxi Formation of middle Permian coals were taken from 7 coalfields of the North China Basin (Fig. 1). These samples are from the Huainan (10), Yanzhou (10), Juye (20), Han-Xing (30), Ningwu (15), Datong (25), and Jungar coalfields (28) (Table 1). Seven in situ coal pillars were randomly sampled from coal mines of the seven coalfields. In situ coal pillars were removed from the coal seam face and wrapped tightly in aluminum foil to retain integrity and orientation. They were cut into small block samples for polishing in laboratory (Fig. 3F).

Macro-Charcoal Analysis

Macro-charcoal was investigated at the mining faces and the pillar samples. Methods of charcoal identification, field collections, and hand specimen recognition of fossil charcoal were described in detail by Scott (2010), whose terminology we follow. At the mining face macro-charcoal shows silky luster. Under a hand lens the charcoal may reveal good anatomical preservation; it is brittle, breaks easily under pressure, and when rubbed may give a black streak. Higher temperature charcoals break more easily. At high temperatures the cell wall may split and begin to fragment. Photographs of macro-charcoal in coal samples are shown in Figure 3.

Petrologic Analysis

The samples were air-dried, crushed to <2 mm, and prepared as epoxy-bound pellets. The petrologic composition was investigated using a Leica DM2500P reflected light microscope equipped with a Craic QDI 302 spectrophotometer at the laboratory of the Key Laboratory of Resource Exploration Research of Hebei Province. The maceral groups were determined by counting 500 points per sample. In the second step, only the fluorescing liptinite macerals were counted under a blue light excitation of 450–490 nm in wavelength. Vitrinite reflectance (R_o) was measured using a Leica DM2500P reflected light microscope that was fitted with a halogen lamp. The measurement was calibrated using a Leitz glass standard (R_{oil} = 0.89%).

Solvent Extraction and Liquid Chromatography

For organic geochemical analyses, samples were Soxhlet-extracted for 48 h using chloroform as solvent. Extract yields were determined gravimetrically after removal of the solvent. The extracts were separated into three fractions [saturated hydrocarbons, aromatic hydrocarbons, and NSO (nitrogen, sulfur, oxygen) compounds] by column chromatography over prewashed silica gel (70–230 mesh, 50 × 1 cm).

Gas Chromatography–Mass Spectrometry

The aromatic hydrocarbon fractions were analyzed at the Key Laboratory for Resource Exploration Research of Hebei Province. Gas chromatography (GC) and gas chromatography–mass spectrometry (MS) analyses of the aromatic fractions were performed on a Hewlett-Packard model 6890 GC coupled to a Hewlett-Packard model 5973 quadrupole mass spectrometric detector. Squalane was added to the aromatic hydrocarbon fractions as internal standards prior to analysis. GC separation was achieved on a DB5-MS fused silica capillary column (30 m × 0.25 mm inner diameter, 0.25 μm film thickness). The GC operating conditions were as follows: temperature held at 60 °C for 5 min, increased from 60 to 300 °C at a rate of 4 °C min^{-1} with final isothermal hold at 300 °C for 15 min. Helium was used as a carrier gas. The sample was injected at a split ratio of 30:1 with the injector temperature at 290 °C. The mass spectrometer was operated in an electron impact mode at 70 eV ionization energy and scanned from 50 to 650 Da. Data were acquired and processed with Chemstation software. Individual compounds were identified through comparisons of mass spectra with literature and library data, along with interpretations of mass spectrometric fragmentation patterns.

Scanning Electron Microscope Analysis

A field-emission scanning electron microscope (SEM) was used to observe the homogenization status of cell walls (Degani-Schmidt et al., 2015). Small fragments of charcoal were sampled from coal specimens with the aid of dissecting needles (with the naked eye or under a Leica DM2500P microscope). The fragments were then mounted on standard stubs with double-sided tape, gold coated, and subsequently examined and photographed with SEM (Hitachi UHR FE-SEM, SU8220) at the Key Laboratory for Resource Exploration Research of Hebei Province.

Zircon U-Pb Analysis

The samples for zircon U-Pb analysis were taken from the Han-Xing Coalfield No. 2 coal seam, which is as much as 4.5 m thick. Zircon grains were separated by conventional magnetic and density techniques to concentrate the nonmagnetic heavy fractions. After sample preparation, zircon grains, free of visible inclusions and major fractures, were hand-picked and embedded in epoxy resin and then polished to expose the grain centers. Cathodoluminescence images were obtained using a NovaTM NanoSem450 electron microprobe in order to characterize the internal structure of the zircons and to select potential target sites for U-Pb analysis.

Zircon U-Pb dating was performed in the Test Center of Shandong Bureau of China Metallurgical Geology Bureau. The zircon grains were ablated in situ with a Coherent Geolas Pro 193nm excimer laser at 10Hz and 10J/cm^2 energy per pulse. The ablation carter diameters were 30 μm,

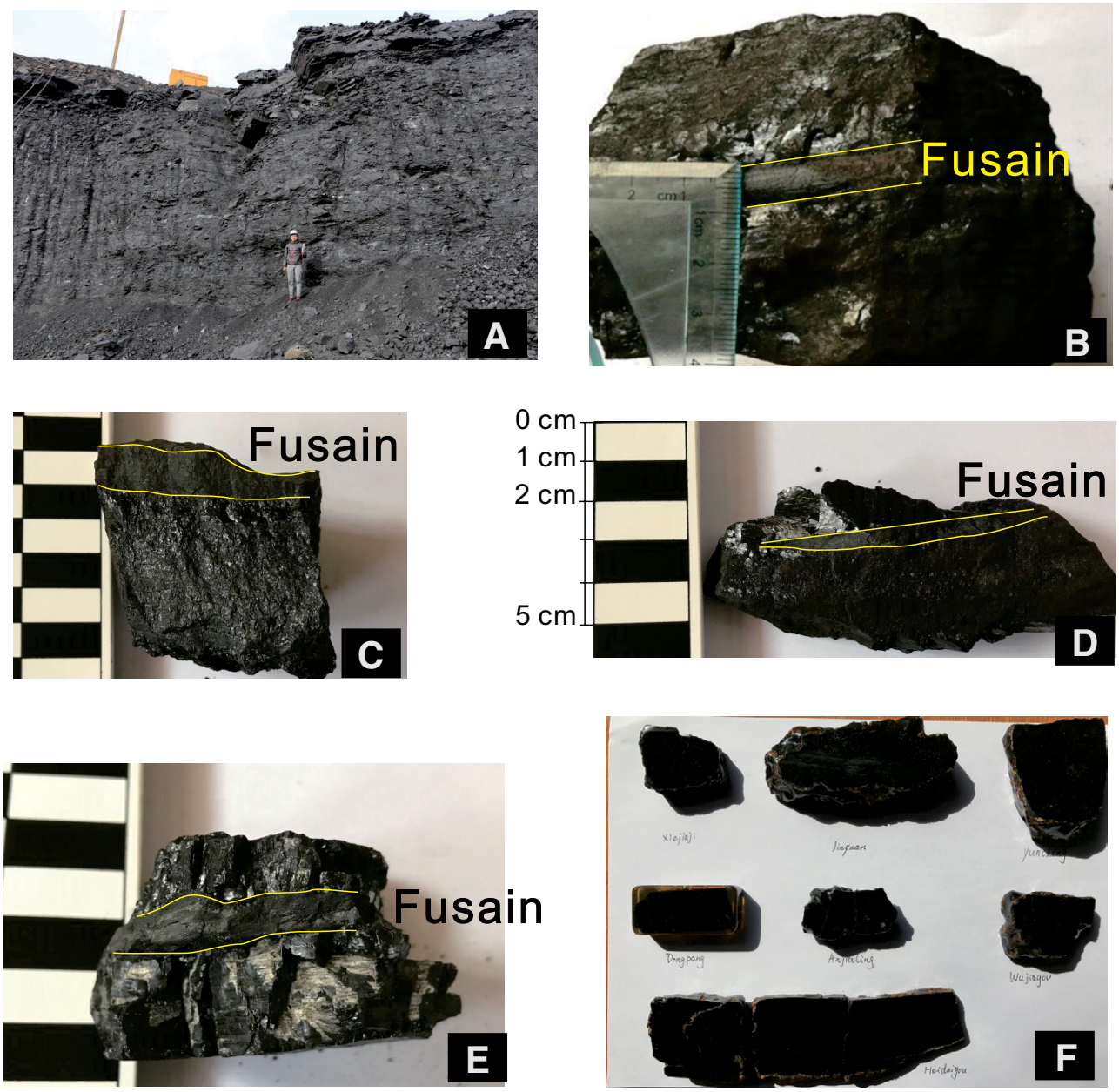

Figure 3. Field and hand sample photographs of fusain layers and in situ pillar samples from the seven coalfields in the North China Basin. (A) General view of studied coal seam at Jungar coalfield. (B) Thin fusain layer of the middle Permian coal from the Han-Xing coalfield. (C) Fusain from the Juye coalfield. (D) Fusain from the Yanzhou coalfield. (E) Fusain from the Datong coalfield. (F) Fusain observed on the polished coal block of Pillar samples from the seven coalfields.

TABLE 1. MACERAL COMPOSITION OF THE COALS FROM THE MIDDLE PERMIAN IN THE NORTH CHINA BASIN

Coalfield	Mine	Sample Amount	Epoch	L total (%)	V total (%)	I total (%)	Charcoal	Coke	R_r (%)
Huainan	Xiejiaji	10	MiddlePermian	5	52	43	yes	yes	0.86
Juye	Yuncheng	10	MiddlePermian	4	56	40	yes	yes	0.71
Yanzhou	Jinyuan	20	MiddlePermian	7	42	51	yes	yes	0.68
Han-xing	Dongpang	30	MiddlePermian	11	44	45	yes	yes	0.66
Datong	Wujiagou	15	MiddlePermian	12	47	41	yes	yes	0.77
Ningwu	Anjialing	25	MiddlePermian	2	51	47	yes	yes	0.62
Jungar	Heigaigou	28	MiddlePermian	8	45	47	yes	yes	0.66

Note: L total—total liptinite, V total—total vitrinite, I total—total inertinite (*sensu* International Committee for Coal and Organic Petrology).

and the sample aerosol was carried to the inductively coupled plasma–mass spectrometer (ICP-MS) by high-purity helium with a flow rate of 0.3 L/min. A ThermoTM iCAPQ ICP-MS was used to analyze the aerosol. Trace element compositions of zircons were calibrated against reference material NIST 610 combined for internal standardization (Liu et al., 2010).

Off-line selection and integration of background and analytic signals, and time-drift correction and quantitative calibration for trace element analyses and U-Pb dating were performed using the ICP-MS DataCal program (http://icpmsdatacal.groups.live.com/). The data processing was described in detail by Liu et al. (2010).

RESULTS

Fusain, Macro-Charcoal, and Meso-Charcoal

Macro-charcoal and meso-charcoal were used as names for large charcoal particles (>180 μm) by Scott (2010). Fusain is now a general term for macroscopic ancient charcoal (Tanner and Lucas, 2016). Fusain, macro-charcoal, and meso-charcoal can be evidence of wildfire (Jasper et al., 2016a). In this study, many fusain as lenticular laminas or isolated particles were observed in the mining faces and hand specimens of seven coal seams (Fig. 3). Abundant macro-charcoal and meso-charcoal horizons have been identified on the polished coal block under microscopy (Figs. 4A, 4B). These charcoal horizons are laterally continuous layers with large discrete clasts of fusinite and semifusinite.

Inertinite (Charcoal)

The definitions of inertinite, charcoal, natural char, and natural coke have been interpreted differently by many scientists and have confused some. The International Committee for Coal and Organic Petrology (ICCP) classified coal metamorphism from peat to rock as four different stages: maceral (including inertinite, vitrinite, and liptinite), natural char, natural coke, and graphite and semigraphite (Kwiecińska and Petersen, 2004). The natural char and natural coke were mainly formed by a relatively local elevated heat flow caused by an intrusive body (Kwiecińska and Petersen, 2004). However, many paleoecologists, paleobotanists, and paleoclimatologists defined most wildfire products as charcoal (including inertinite and natural char, sensu ICCP; see Kwiecińska and Petersen, 2004; Scott, 2010; Robson et al., 2015). By comparison with these different definitions, it can be found that charcoal is referred to as inertinite in the petrographic study of coals (Sýkorová et al., 2005; Scott, 2010). In this study inertinite follows the definition by the ICCP (2001) and charcoal is defined as in Scott (2010).

Maceral compositions of the middle Permian coal samples (the No. 2 seam) from seven coalfields in the North China Basin were measured; their proportions are shown in Table 1, and the photomicrographs of the inertinites are shown in Figures 4A–4D. The liptinite contents are very low and vary from 2% to 12%. The vitrinite contents vary from 42% to 56%. The average proportions of inertinite in the coal samples range from 40% to 51%. The most abundant inertinite macerals are semifusinite and inertodetrinite with minor fusinite. Two types of cell walls were observed under SEM, lamellar cell walls and homogenized cell walls (Figs. 5A, 5B). These cell walls confirmed the categorization of the material as charcoal (Degani-Schmidt et al., 2015). Due to high compression after burial, the cell walls are fractured (Figs. 4A, 5A, and 5B).

Natural Char

"Natural char is formed by the influence of heat from fire on (1) coal or (2) gelified organic matter in a peat" (Kwiecińska and Petersen, 2004, p. 113). Natural char (sensu ICCP) shows black components and its reflectance is typically higher than the reflectance of the associated inertinite (Kwiecińska and Petersen, 2004). Natural char could be formed by both volcanic events and wildfires (Kwiecińska and Petersen, 2004; Scott, 2010). According to Scott (2010), the natural char formed by wildfire is classified as charcoal. Abundant natural char (sensu ICCP) particles have been observed in the Permian coal samples from all coalfields investigated in this study, visible as isolated particles in coal seams (Fig. 4E). These particles exhibit many pores under the reflected light microscope; this is typical of natural char (sensu ICCP) according to Kwiecińska and Petersen (2004). Under SEM, natural char (sensu ICCP) shows homogenized cell walls (Fig. 5B).

Natural Coke

Natural coke was defined as coke formed by wildfires (China National Administration of Coal Geology, 1996). In this study, some isolated coke particles were observed in the Permian coals (Fig. 4F). Under SEM, these coke particles exhibit pores and plastic deformation, which is a feature typical of natural coke (sensu ICCP; see Kwiecińska et al., 1992). These particles are distributed along the microlayers.

Polycyclic Aromatic Hydrocarbons

Polycyclic aromatic hydrocarbon (PAH) fractions of the middle Permian coals from seven mines of the North China Basin were analyzed by GS-MS methods. The notable high-molecular-weight four-ring aromatics are (1) pyrene, (2–4) methylfluoranthenes, (5) benzo(a)anthracene, and (6) triphenylene + chrysene, whereas the notable five-ring aromatics are (7) benzo(k)fluoranthene + benzo(b)fluoranthene, (8) benzo(a)pyrene, (9) benzo(e)pyrene, and (10) perylene. Among the heavier PAHs (more than five-ring) identified, (11) indeno[1,2,3-cd]pyrene and (12) benzo(ghi) perylene are abundant, whereas (13) coronene is only found in the coal samples from the Jungar coalfield (Fig. 6; Table 2).

Radiometric Age Determination

We analyzed 43 zircon grains of the coal samples from the No. 2 seam of the Dongpang coal mine, Han-Xing coalfield, for U-Pb radiometric dating. Three age populations can be defined: (1) 2534–1357 Ma with a major peak at 1970 Ma, (2) 426–300 Ma with a major peak at 333 Ma, and (3) 297–252 Ma with a peak at 274.9 Ma. The old population ages of 2534–1357 Ma and 426–300 Ma should be from the provenance highland around the coal basin. The concordia (mean square of weighted deviates, MSWD = 2.5) plots of 22 younger grains show an age cluster near the intercept at 273 ± 13 Ma and a weighted mean age of 272.7 ± 4.7 Ma (95% confidence, MSWD = 4.5) (Figs. 7A, 7B). These results indicate that the No. 2 coal seam was formed ca. 270 Ma.

DISCUSSION

Origin of Inertinite, Natural Char, and Natural Coke

Origin of Inertinite

To better understand charcoal, the definition of inertinite (sensu ICCP) is briefly reviewed here. Inertinite is a maceral group of coal, characterized by a higher reflectance than the associated vitrinite and liptinite macerals (ICCP, 2001). It is chemically characterized by a higher degree of aromatization in the macromolecular structure and relatively low hydrogen content compared to the other macerals. Diessel (2010) reviewed and

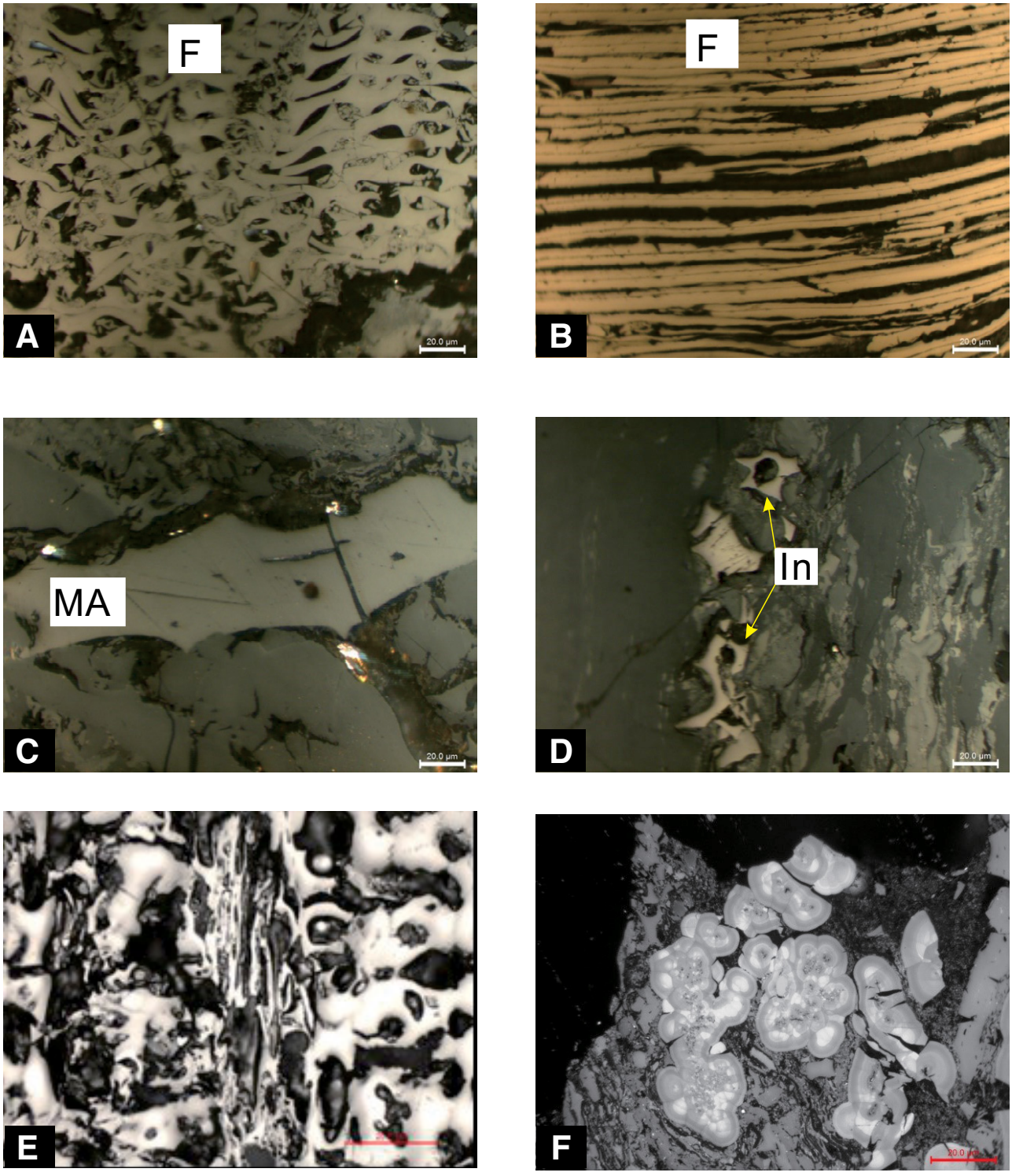

Figure 4. Photomicrographs of inertinite (sensu International Committee for Coal and Organic Petrology, ICCP), natural char (sensu ICCP) and natural coke from the North China Basin. (A) Fusinite (F; charcoal horizon) from Han-Xing coalfield. (B) Fusinite (charcoal horizon) from Datong coalfield. (C) Macrinite (MA; sensu ICCP; macroscopic charcoal) from Juye coalfield. (D) Inertodetrinite (In; sensu ICCP; microscopic charcoal) from Yanzhou coalfield. (E) Natural char (sensu ICCP) from Datong coalfield (scanning electron microscope photograph). (F) Natural coke from Jungar coalfield (scanning electron microscope photograph).

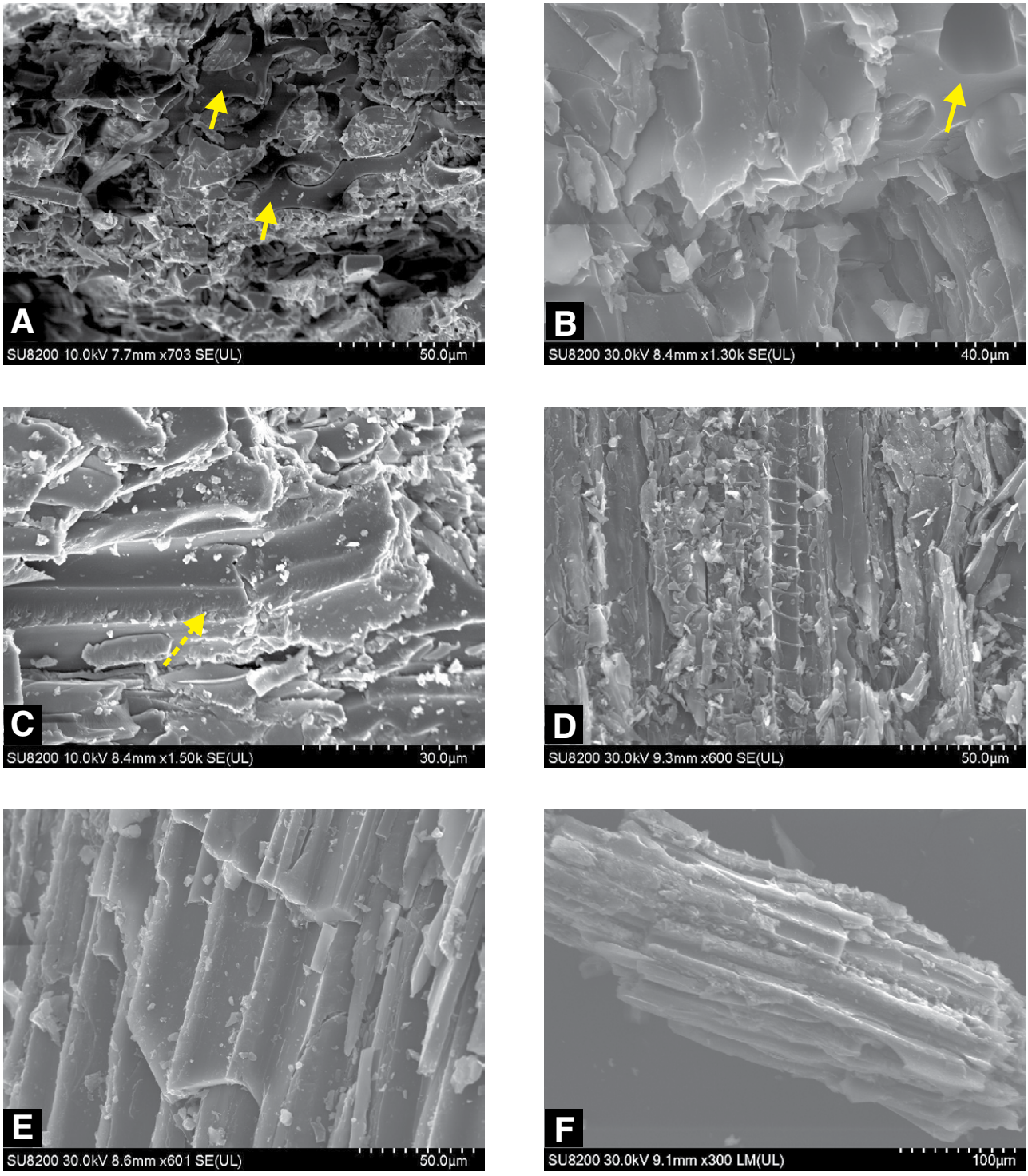

Figure 5. Scanning electron microscope micrographs of inertinite (charcoal) in the No. 2 Coal of the Shanxi Formation from the North China Basin. (A, B) Cross section of charcoal; cell walls are homogenized (solid yellow arrows). (C) Longitudinal section of charcoal; cell walls are inhomogeneous (dashed yellow arrow). (D) Longitudinal section of charcoal; secondary wood anatomy is preserved as charcoal. (E) Axial section of cell wall. (F) Oblique section of cell wall.

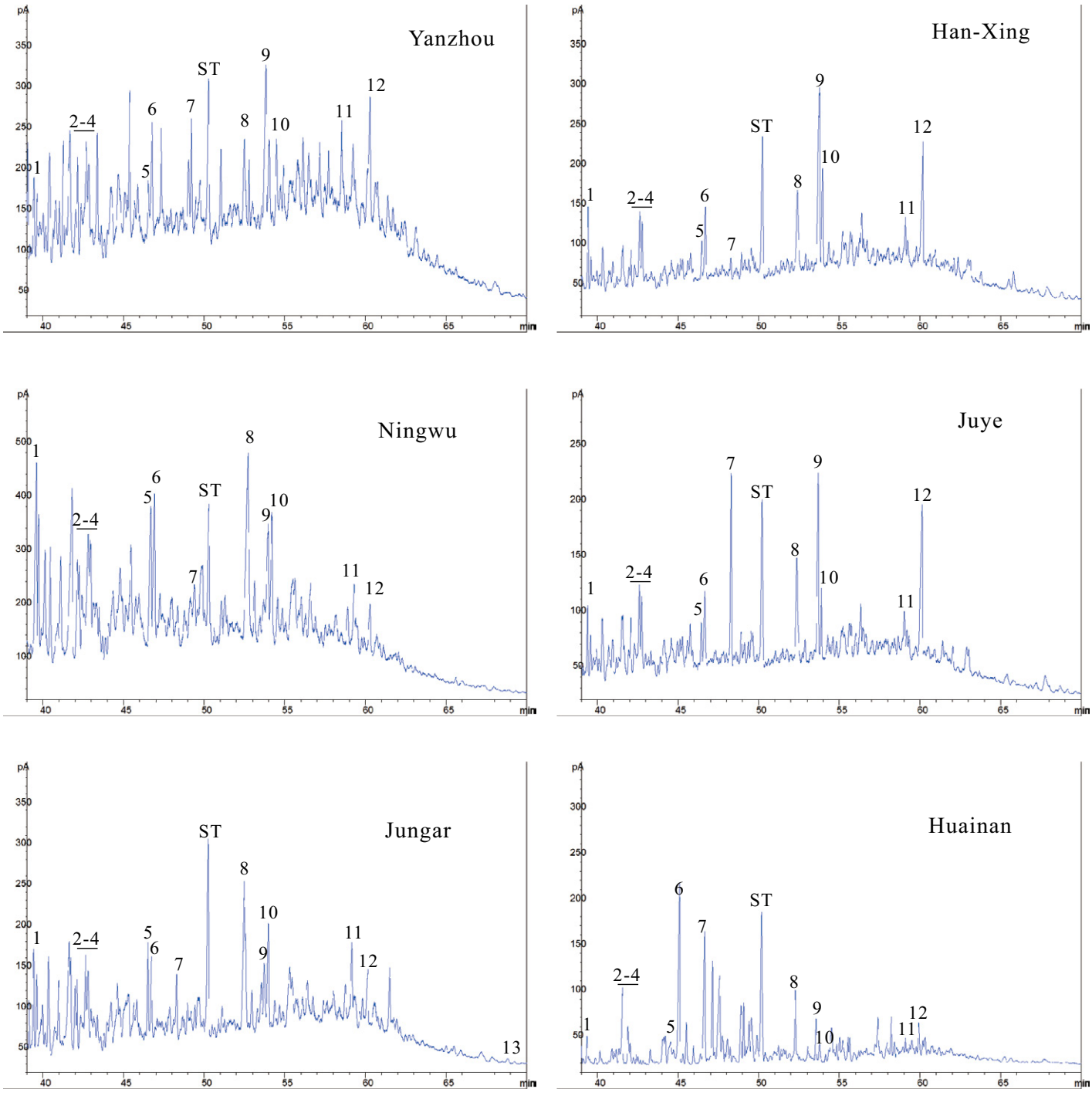

Figure 6. Gas chromatograms of aromatic hydrocarbon fractions of middle Permian coal. For assignment of peak numbers to individual compounds, see Table 2. ST—standard.

TABLE 2. MOLECULAR FORMULA, WEIGHT, AND STRUCTURE OF THE IDENTIFIED FOUR-, FIVE- AND SIX-RING PYROGENIC POLYCYCLIC AROMATIC HYDROCARBONS OF THE MIDDLE PERMIAN COAL SAMPLES FROM THE NORTH CHINA BASIN

Peak	Compound name	Molecular formula	Molecular weight	Molecular structure
1	pyrene	$C_{16}H_{10}$	202	
2	methylfluoranthene	$C_{17}H_{12}$	216	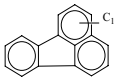
3	methylfluoranthene	$C_{17}H_{12}$	216	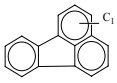
4	methylfluoranthene	$C_{17}H_{12}$	216	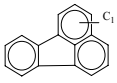
5	benzo(a)anthracene	$C_{18}H_{12}$	228	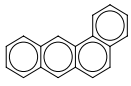
6	triphenylene+chrysene	$C_{18}H_{12}$	228	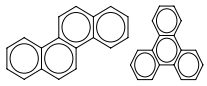
7	benzo(k)fluoranthene + benzo(b)fluoranthene	$C_{20}H_{12}$	252	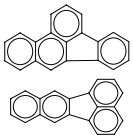
8	benzo(a)pyrene	$C_{20}H_{12}$	252	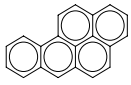
9	benzo(e)pyrene	$C_{20}H_{12}$	252	
10	perylene	$C_{20}H_{12}$	252	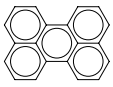
11	Indeno(1,2,3-cd)pyrene	$C_{22}H_{12}$	276	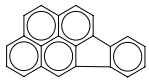
12	benzo(ghi)perylene	$C_{22}H_{12}$	276	
13	coronene	$C_{24}H_{12}$	300	

discussed inertinite (charcoal) in detail. High percentages of inertinite macerals in coals were formerly thought to originate from postdepositional oxidation of wood. However, according to later studies, inertinite could also be formed by fires (Bustin, 1997). Most inertinite macerals were explained as originating from wildfire activity (Scott and Glasspool, 2006, 2007; Diessel, 2010; Hudspith et al., 2012; Glasspool and Scott, 2013; Jasper et al., 2016a); however, Hower et al. (2013) argued that wildfire is not the only path to the formation of inertinite macerals, and degradation of organic matter could also be a pathway for inertinite formation. In this study we agree with the viewpoint of Scott and Glasspool (2006). The high inertinite ratios in this study indicate that wildfires occurred during the middle Permian Period in the North China Basin. "Bogen-struktur" (arc-shaped structure) produced by shattering of the cell walls are present (Fig. 4A), indicating high compaction of the tissues (Degani-Schmidt et al., 2015).

Natural Char

According to Kwiecińska and Petersen (2004), natural char has a higher reflectance than the associated huminite and/or vitrinite and inertinite macerals, and is characterized by a distribution of pores and varying porosity. Recent studies indicate that this kind of natural char (sensu ICCP) is also charcoal (Scott, 2010; Degani-Schmidt et al., 2015; Jasper et al., 2016b). Scott and Glasspool (2006) concluded that charcoal can be equated with the inertinite group macerals. Scott and Glasspool (2007) and Glasspool and Scott (2013) stated that inertinite is synonymous with charcoal, and is almost exclusively considered to be formed as a byproduct of wildfires.

In this study natural char (sensu ICCP) was characterized by a random distribution of pores and a varying porosity with a reflectance higher than the associated inertinite. These natural char particles in coals from the North China Basin could have been formed by wildfires or as a result of volcanic activity and long-range transport by water and/or wind. The closest continent for the North China Basin is the South China block (Fig. 1). There was no coal formed (Han and Yang, 1980) and major wildfires were unlikely in south China in the middle Permian Period. There is also no evidence available for the transport of natural char from outside into the North China Basin. Therefore, charcoal in the North China Basin could not be transported from south China into the basin, and should have been autochthonously formed by wildfires.

Hudspith et al. (2012) interpreted the wildfire types according to the size of charcoal particles and their reflectance. Charcoal horizons are considered to represent charred vegetation from surface fire events; macro-charcoal may have been transported locally by wind under particular conditions or more commonly by water transport through overland flow; microscopic charcoal (<180 µm but more commonly <20 µm) is generally interpreted as the wind-borne size fraction from regional, particularly crown fire events within 20–100 km of the fire source (Hudspith et al., 2012). In this study, all charcoal horizons, macro-charcoal particles, and microscopic charcoal particles were observed (Figs. 4A–4D), but most charcoals belong to charcoal horizons, the microscopic charcoal particles are secondary, and the macro-charcoal particles are at a minimum. This phenomenon may indicate that surface fire events are the main wildfire type, and crown fire events are secondary. Charcoal horizons also proved that charcoal has been formed autochthonously by wildfires (Hudspith et al., 2012).

According to Scott (2010), the lamellar cell walls of charcoal were formed at a temperature of 300 °C and homogenized cell walls were formed at >300–325 °C. Therefore, two types of cell wall observed in this study may indicate the occurrence of wildfires at temperatures of both 300 and >325 °C.

Natural Coke

In this study, coke particles exist in coal seams as isolated particles. The coke particles are distributed along the microlayers, which may indicate that these coke particles were formed during a sedimentation stage. This type of coke is different from massive coke, which formed from coal through alteration by a relatively local elevated heat flow from an intrusive body that showed forms of discordant and concordant bodies (Kwiecińska and Petersen, 2004). There are no intrusive bodies recorded in the coal mines, where samples have been collected. Therefore, we suggest that these coke particles formed by extremely high temperature wildfires. The organic matter was buried and incomplete combustion occurred, resulting in the formation of the coke particles. The China National Administration of Coal Geology (1996) also found some natural coke particles in middle

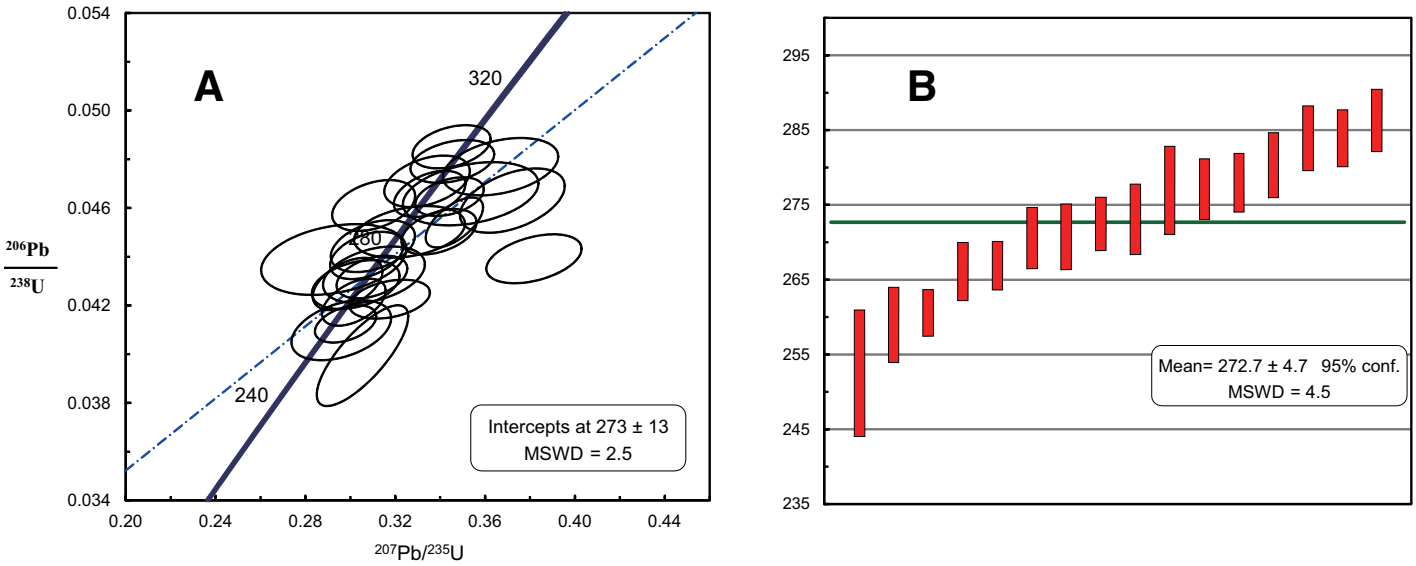

Figure 7. Results of U-Pb radiometric dating of zircon from the coal roof and parting samples of the Han-Xing coalfield. (A) U-Pb concordia plot (2σ error) of zircons. (B) Mean age plot (1σ error) of zircons. MSWD—mean square of weighted deviates; conf.—confidence.

Permian coals from eight coalfields in the North China Basin but did not discuss the possible formation mechanism. The abundance of coke particles found in our study further confirms the occurrence of widespread wildfires in the North China Basin in this period.

Origin of High-Molecular-Weight Aromatic Compounds

PAHs can have various origins ranging from petrogenic (diagenesis of sedimentary organic matter) to pyrogenic (combustion of organic matter) (Freeman and Cattell, 1990). The relatively high intensities of benzo(a)pyrene and benzo(ghi)perylene in the aromatic hydrocarbon fractions suggest that the PAHs in the Permian coal are pyrolytic products that originated from either forest fires or volcanic activity (Geptner et al., 2002; van de Schootbrugge et al., 2009). PAHs can be formed through the spontaneous combustion of coal below the subsurface (Shen et al., 2011; Freeman and Cattell, 1990; Scott and Glasspool, 2006). However, there is no evidence for spontaneous underground coal combustion in the sampled coal mines. Therefore, the PAHs must have been formed in geological history through the combustion of natural vegetation or peat layers.

To study the origin and formation mechanism of the PAHs, coal samples from both the Carboniferous and middle Permian Period were taken from the same coal mine (Dongpang mine, Han-Xing coalfield). The mean vitrinite reflectance value of the Carboniferous coal is 0.27% higher than that of the middle Permian coal from the same section (Sun et al., 2002). Thus, the amount of PAHs in the Carboniferous coal should be higher than in the Permian coal because the Carboniferous coal went through a higher geothermal regime associated with a longer period of time at elevated temperature. The composition of the PAHs of the middle Permian coal is completely different compared to the Carboniferous coal with high-molecular-weight PAHs present only in the middle Permian coal samples (Fig. 6; Sun et al., 2002). The presence of high-molecular-weight PAHs in the middle Permian coals is not explainable by regular geothermal effects, but rather by vegetation wildfires during the swamp and/or peat forming stage (Shen et al., 2011). Therefore, the inertinite macerals in the middle Permian coals are suggested to be associated with the occurrence of wildfires. Aromatic hydrocarbon fractions of the Carboniferous coal samples from Han-Xing coalfield were studied by Sun et al. (2002), and the heavier PAHs (more than five-ring) were not found. The chromatograms of aromatic hydrocarbon fractions obtained from the extracts of the Carboniferous coal samples in this study are similar to those obtained from Carboniferous coals from the Xingtai coalfield studied previously (Sun et al., 2002). PAHs with more than four condensed rings are not detectable in these extracts. However, in the Permian coal from the No. 2 seam in the Dongpang mine from the Xingtai coal field, PAHs with more than four condensed rings were detected in association with many other aromatic hydrocarbons such as naphthalene, phenanthrene, dibenzofurane, dibenzothiophene, and their alkylated derivatives (Sun et al., 2002). In the previous study it was not yet recognized that the occurrence of PAHs such as pyrene, chrysene bebenzo(k)fluoranthene + benzo(b)fluoranthene, benzo(a)pyrene, and benzo(e)pyrene might be regarded as indicators for wildfires in the middle Permian.

Relationship of Atmospheric Oxygen Concentration and Wildfire Events

Atmospheric oxygen levels are presumed to have changed dramatically during Earth history (Bergman et al., 2004; Scott and Glasspool, 2006; Berner, 2009; Belcher et al., 2010a). The O_2 levels in the early-Late Devonian Epoch have been suggested to have been as low as 13% (Berner, 2006). The levels increased during the Carboniferous and Permian, peaking at 30% in the early Guadalupian Epoch (ca. 270 Ma) (Berner, 2006, 2009). These fluctuations are suspected of having a dramatic effect on the development of fire systems (Belcher and McElwain, 2008; Shi and Waterhouse, 2010; Glasspool et al., 2015). According to Belcher et al. (2010b), Earth's highest fire frequencies under current levels of O_2 are mainly in equatorial dry areas and seasonally dry climates; if O_2 significantly increased >25%, even swamp and wet areas would burn, so that fire frequencies would be increased in both tropical rainforest and arctic tundra. According to an inertinite ratio–O_2 level calculation curve (Glasspool et al., 2015), O_2 levels reached ~27% in the middle Permian in the North China Basin; therefore, O_2 levels of 27% could have caused widespread wildfires in the basin. The O_2 levels gradually decreased from

270 to 260 Ma, and then dramatically decreased from 260 to 250 Ma (Fig. 2F) (Bergman et al., 2004; Berner, 2006). The gradual decrease of O_2 could have consumed by the occurrence of global wildfires (Singh and Shukla, 2004; Jasper et al., 2013; Manfroi et al., 2015; Kauffmann et al., 2016), also affecting the North China Basin (Scott and Glasspool, 2006; Glasspool et al., 2015).

Experimental data also provide the following observations on O_2 levels and fire in the fossil record: fire activity would be greatly suppressed below 18.5% O_2, and entirely stopped below 16% O_2 (Belcher et al., 2010b); between 18% and 23% fire occurrences would have been similar to those under the present atmospheric level (PAL) of 21% (Pyne et al., 1996); at a level of 25% O_2 in the atmosphere, fires would have been widespread (Wildman et al., 2004); and fire activity would have been globally distributed at O_2 levels over 25% (Belcher et al., 2010b) or levels of 30% (Wildman et al., 2004). In the middle Permian, global O_2 levels should have been >27% (Berner, 2006, 2009), and caused global wildfire; therefore, wildfires in the North China Basin might have been only a part of the global wildfires during that period (Wang and Chen, 2001; Yan et al., 2016). Data from a total of 2989 coal samples collected worldwide were summarized by Glasspool et al. (2015). Their inertinite contents were calculated and divided into different groups according to the coal age (Table 3). Comparison of the inertinite contents in Permian coals from north China with coals from all other places in the world shows a similar distribution trend (Table 3). The highest inertinite contents of Permian coals reach 44.95% and 46.2%, respectively. These values are equivalent to the (~42%) reported occurrences of inertinites and/or black carbon in the Permian by Abu Hamad et al. (2012) and the values (9%–70%) reported content of inertinites in the Permian by Diessel (2010). These data may indicate that wildfires in the Permian are global events. Before and after the Permian, the inertinite contents of coals decrease sharply (Table 3).

Volcanic Eruption Events

Higher atmospheric oxygen levels during the Permian Period led to a doubling of ignition potential of vegetation (Jasper et al., 2016a); thus, wildfires were far more prevalent than in the present day. However, the wildfires would have been ignited by some events, such as lightning, or abundant local volcanic eruptions. In the middle Permian there were also some local volcanic eruptions in north China (Zhao et al., 2010). The collision of the North China block with Siberia during the Permian and the Sino-Mongolian seaway closing during the middle Permian resulted in abundant volcanism along the northern margin of north China during this period (Zhao et al., 2010; Stevens et al., 2011). Therefore, these middle Permian eruptions in north China could also have ignited wildfires. For example, late Paleozoic volcanism existed along the eastern margin of the North China plate, which was formed by the South and North China plates colliding along the eastern margin of the North China plate (Zhang, 1997). The areal distribution of the igneous rock is >10,000 km^2; we designate this as the Luxi igneous rock province (LIRP). The LIRP erupted from the late Carboniferous and eruption ended in the late Permian (Zhang, 1997). In the Shanxi Formation, the thickness of igneous rocks reaches 61 m and tephra can be observed in the coal partings (Zhang, 1997). This phenomenon may indicate that the volcanism occurred during the peat formation. The Yanzhou coalfield is located close to this area and the distance from the Han-Xing coalfield to the LIRP is only 200 km. Therefore, the wildfires could have ignited by local volcanism.

TABLE 3. INERTINITE (CHARCOAL) CONTENTS OF COALS FROM NORTH CHINA AND THE WORLD

World*			
Period	Age (Ma)	Number of samples	Average inertinite† (mmf %)
Triassic	201.6–251	32	2.47
Permian	251–299	1612	44.95
Carboniferous	299–359	1397	19.27
Devonian	359–385	48	11.61
North China			
Period	Age (Ma)	Number of samples	Average inertinite (mmf %)
Triassic	201.6–251	13	23.67 (Zhou et al., 2015)
Permian	251–299	29	46.2 (Dai et al., 2008)
Carboniferous	299–359	9	17.0 (Dai et al., 2015)
Devonian	359–385	1	14.28 (Cheng, 2006)

*Calculated according to original data by Glasspool et al. (2015).
†mmf—mineral matter free.

Pollutant Release from Wildfires

It is generally accepted that flood basalt provinces played a very important role for the five largest mass extinctions in Earth history (Courtillot and Renne, 2003; Wignall et al., 2009; Bond et al., 2010; Bond and Wignall, 2014) and were linked to extreme greenhouse warming, which in turn was triggered by the release of carbon dioxide from flood basalt volcanism (Beerling and Berner, 2002). Van de Schootbrugge et al. (2009) suggested that the release of pollutants such as sulfur dioxide and toxic compounds such as the PAHs may have contributed to the extinction at the Triassic-Jurassic boundary, because the terrestrial vegetation shift during this mass extinction event was so severe and wide ranging that it is unlikely to have been triggered by greenhouse warming alone.

The inertinite contents in the upper Permian coals from south China are lower than 20% (Zhong and Smyth, 1997), whereas they reach 40%–51% in the middle Permian coals from the North China Basin (Table 1). These observations may indicate that the wildfires in the middle Permian Period were more widespread than during the late Permian Period in south China. It has been proved that combustion, particularly incomplete combustion of vegetation and organic matter in peat, enabled the massive production of carbon dioxide, carbon monoxide, sulfur dioxide, methane, and PAHs, and their release to the aerosphere by the end-Permian Siberian Traps and Longwood-Bluff intrusions of New Zealand (Wang et al., 1985; van de Schootbrugge et al., 2009). The wildfires of the middle Permian Period in the North China Basin could have also released an enormous amount of harmful gases, because the basin is a megacoalfield with an area of 800,000 km^2. Widespread wildfires in such a megacoalfield could discharge enormous amount of harmful gases and increase ambient temperatures. The pollutant discharge and the concomitant temperature increase might have affected floral growth thereafter. According to Stevens et al. (2011), three floral extinction events in north China in the lower Shihhotse Formation (upper-middle Permian Period), which directly overlies the Shanxi Formation, have been found. Therefore, we may deduce that enormous amount of harmful gases released and increased local temperatures could be one of the reasons for the floral extinctions that occurred after the time of the Shanxi Formation.

Time Framework for the Wildfires

The geochronology, lithostratigraphy, and biostratigraphy of the North China Basin have been studied since the early 1900s (Norin, 1922; China National Administration of Coal Geology, 1996; Wang, 2010; Stevens et al., 2011). It is notoriously difficult to determine the stratigraphy of

Carboniferous and Permian terrestrial sequences in north China because of a lack of appropriate marine species for high-resolution biostratigraphy in most cases (Wang, 2010; Stevens et al., 2011). For example, fossil plant biostratigraphy offers the potential to correlate fossiliferous sequences within single basins, but on a regional scale this is more problematic and provides only a basic level of correlation (Wang, 2010; Stevens et al., 2011). Therefore, this issue has been unresolved (National Committee of Stratigraphy of China, 2014). Paleomagnetic data can serve as a viable method for sequence stratigraphy (Isozaki, 2009). However, after the late Carboniferous and ending in the middle Permian, only one stable interval (Kiaman Reverse Superchron) was observed (Isozaki, 2009) and is not able to provide stratigraphic information on the Cisuralian and the early Guadalupian sequence. Recent studies show that the U-Pb age spectra of detrital zircons obtained from clastic sedimentary rocks can provide important constraints for reconstruction of the time framework of geological evolution (Richards et al., 2005; Yang et al., 2006); Veevers et al. (2005) pointed out that U-Pb ages of detrital zircons can provide the maximum age for sedimentary rocks.

Fossil plant evidence indicates that the Shanxi Formation is of Sakmarian–Artinskian age within the Cisuralian (Fig. 2A), but it also may extend into the late Kungurian (Wang, 2010). The latest U-Pb ages of the detrital zircons, which are from the standard stratotype section of the late Paleozoic coal-bearing strata of north China, give the minimum and maximum age of 262 Ma and 271 ± 7 Ma, respectively, for the Shanxi Formation (Sun et al., 2014). Based on the U-Pb ages and Hf isotopic data, Yang et al. (2006) determined a minimum age of 262 ± 2 Ma in one sandstone sample from the middle Shanxi Formation that differs slightly from the results obtained from our study (Fig. 7). The 262 Ma age would coincide with the Capitanian extinction manifested from marine sediments at Boreal latitudes in Spitsbergen (Bond et al. 2015). Considering the references mentioned herein and our data, it can be concluded that the No. 2 coal seam was formed during Roadian (ca. 270 Ma). Therefore, it is inferred further that the wildfire could have been widespread in the North China Basin ca. 270 Ma. The O_2 levels gradually decreased from 270 Ma on due to consumption by wildfires (Fig. 2F). Stevens et al. (2011) recognized three floral extinctions in the Permian continental sequences from North China Basin (Fig. 2E). According to the lithostratigraphy, the strata, in which three floral extinctions occurred, belong to the lower Shihhotse Formation (Fig. 2E), which overlies the Shanxi Formation (Stevens et al., 2011). However, according to a geochronological chart (Figs. 2A, 2B), the geochronological data (ca. 270 Ma) given by Stevens et al. (2011), in which the earliest floral extinction occurred, belong to the earlier middle Permian (Stevens et al., 2011). Therefore, the time of the earliest floral extinction is correlated with the major wildfire event (Figs. 2D, 2E). The vegetation of the Shanxi Formation and thereafter the lower Shihhotse Formation, could have been influenced by releases of massive quantities of carbon dioxide, carbon monoxide, sulfur dioxide, methane, and PAHs produced by wildfires into the atmosphere.

CONCLUSIONS

This study indicates that wildfires were widely prevalent during the middle Permian Period in the North China Basin. These could have produced a significant amount of gases, PAHs, fossil charcoal, and coke particles. The presence of high-molecular-weight aromatic hydrocarbons detected in middle Permian coals from the North China Basin indicates that PAHs formed through the combustion of natural vegetation or peat during its formation. The presence of high concentrations of charcoal and natural coke particles also indicates that the precursor mires and peats of the middle Permian coal from the North China Basin underwent far-ranging wildfires. These wildfires could have been ignited by lightning or volcanic eruptions in north China.

These wildfires could have consumed enormous amounts of O_2 from the atmosphere; the middle Permian coals are the largest coal reserves in China, in which the fossil charcoal reached proportions between 40% and 51% of the coals. The wildfires could also have discharged massive quantities of pollutants and increased ambient temperatures. Both the pollutant discharge and the increasing temperatures could be the reasons for the floral extinctions that occurred during the middle Permian.

ACKNOWLEDGMENTS

This research was supported by the National Natural Science Foundation of China (grants 41330317 and 41641019). We thank Qiaojing Zhao, Bangjun Liu, Jialiang Ma, and Weixu Li for their help in sampling and laboratory work.

REFERENCES CITED

Abu Hamad, A.M.B., Jasper, A., and Uhl, D., 2012, The record of Triassic charcoal and other evidence for palaeo-wildfires: Signal for atmospheric oxygen levels, taphonomic biases or lack of fuel?: International Journal of Coal Geology, v. 96–97, p. 60–71, doi:10.1016/j.coal.2012.03.006.

Beerling, D.J., and Berner, R.A., 2002, Biogeochemical constraints on the Triassic-Jurassic boundary carbon cycle event: Global Biogeochemical Cycles, v. 16, p. 11–13, doi:10.1029/2001GB001637.

Belcher, C.M., and McElwain, J.C., 2008, Limits for combustion in low O_2 redefine paleoatmospheric predictions for the Mesozoic: Science, v. 321, p. 1197–1200, doi:10.1126/science.1160978.

Belcher, C.M., Mander, L., Rein, G., Jervis, F.X., Haworth, M., Hesselbo, S.P., Glasspool, I.J., and McElwain, J.C., 2010a, Increased fire activity at the Triassic/Jurassic boundary in Greenland due to climate-driven floral change: Nature Geoscience, v. 3, p. 426–429, doi:10.1038/ngeo871.

Belcher, C.M., Yearsley, J.M., Hadden, R.M., McElwain, J.C., and Rein, G., 2010b, Baseline intrinsic flammability of Earth's ecosystems estimated from paleoatmospheric oxygen over the past 350 million years: National Academy of Sciences Proceedings, v. 107, p. 22448–22453, doi:10.1073/pnas.1011974107.

Belcher, C.M., Collinson, M.E., and Scott, A.C., 2013, A 450 million year record of fire, *in* Belcher, C.M., ed., Fire phenomena and the Earth system—An interdisciplinary approach to fire science: Chichester, UK, John Wiley and Sons Ltd, p. 229–249.

Bergman, N.M., Lenton, T.M., and Watson, A.J., 2004, COPSE: A new model of biogeochemical cycling over Phanerozoic time: American Journal of Science, v. 304, p. 397–437, doi:10.2475/ajs.304.5.397.

Berner, R.A., 2006, GEOCARBSULF: A combined model for Phanerozoic atmospheric O_2 and CO_2: Geochimica et Cosmochimica Acta, v. 70, p. 5653–5664, doi:10.1016/j.gca.2005.11.032.

Berner, R.A., 2009, Phanerozoic atmospheric oxygen: New results using the GEOCARBSULF model: American Journal of Science, v. 309, p. 603–606, doi:10.2475/07.2009.03.

Bond, D.P., and Wignall, P.B., 2014, Large igneous provinces and mass extinctions: An update, *in* Keller, G., and Kerr, A.C., eds., Volcanism, impacts, and mass extinctions: Causes and effects: Geological Society of America Special Paper 505, p. 29–55, doi:10.1130/2014.2505(02).

Bond, D.P.G., Hilton, J., Wignall, P.B., Ali, J.R., Stevens, L.G., Sun, Y.D., and Lai, X.L., 2010, The Middle Permian (Capitanian) mass extinction on land and in the oceans: Earth-Science Reviews, v. 102, p. 100–116, doi:10.1016/j.earscirev.2010.07.004.

Bond, D.P.G., Wignall, P.B., Joachimski, M.M., Sun, Y., Savov, I., Grasby, S.E., Beauchamp, B., and Blomeier, D.P.G., 2015, An abrupt extinction in the Middle Permian (Capitanian) of the Boreal Realm (Spitsbergen) and its link to anoxia and acidification: Geological Society of America Bulletin, v. 127, p. 1411–1421, doi:10.1130/B31216.1.

Bustin, R.M., 1997, Cold temperate peats and coals: Their sedimentology and composition, *in* Martini, I.P., eds., Late glacial and postglacial environmental changes, Quaternary, Carboniferous–Permian and Proterozoic: New York, Oxford University Press, 343 p.

Cheng, D.S., 2006, Organic geochemical characteristics of Chinese Devonian coal: Coal Geology of China, v. 18, p. 7–10 (in Chinese with English abstract).

China National Administration of Coal Geology, 1996, Atlas for coal petrography of China: Xuzhou, China University of Mining and Technology, 321 p.

Courtillot, V.E., and Renne, P.R., 2003, On the ages of flood basalt events: Comptes Rendus Geoscience, v. 335, p. 113–140, doi:10.1016/S1631-0713(03)00006-3.

Dai, F.G., Liu, B.R., and Yang, K.S., 2008a, Geological interpretation of seismic sections and tectonic evolution of the North China basin: Geology in China, v. 35, p. 820–840 (in Chinese with English abstract).

Dai, S.F., Li, D., Chou, C.L., Zhao, L., Zhang, Y., Ren, D.Y., Ma, Y.W., and Sun, Y.Y., 2008b, Mineralogy and geochemistry of boehmite-rich coals: New insights from the Haerwusu Surface Mine, Jungar Coalfield, Inner Mongolia, China: International Journal of Coal Geology, v. 74, p. 185–202, doi:10.1016/j.coal.2008.01.001.

Dai, S.F., et al., 2015, Mineralogical and geochemical compositions of the Pennsylvanian coal in the Hailiushu Mine, Daqingshan Coalfield, Inner Mongolia, China: Implications of sediment-source region and acid hydrothermal solutions: International Journal of Coal Geology, v. 137, p. 92–110, doi:10.1016/j.coal.2014.11.010.

Degani-Schmidt, I., Guerra-Sommer, M., Mendonç, J. de O., Filho, J.G.M., Jasper, A., Cazzulo-Klepzig, M., and Iannuzzi, R., 2015, Charcoalified logs as evidence of hypautochthonous/autochthonous wildfire events in a peat-forming environment from the Permian of southern Paraná Basin (Brazil): International Journal of Coal Geology, v. 146, p. 55–67, doi:10.1016/j.coal.2015.05.002.

Diessel, C.F.K., 2010, The stratigraphic distribution of inertinite: International Journal of Coal Geology, v. 81, p. 251–268, doi:10.1016/j.coal.2009.04.004.

DiMichele, W.A., Montañez, I.P., Poulsen, C.J., and Tabor, N.J., 2009, Climate and vegetational regime shifts in the late Paleozoic ice age earth: Geology, v. 7, p. 200–266, doi:10.1111/j.1472-4669.2009.00192.x.

Flannigan, M.D., Krawchuk, M.A., de Groot, W.J., Wotton, B.M., and Gowman, L.M., 2009, Implications of changing climate for global wildland fire: International Journal of Wildland Fire, v. 18, p. 483–507, doi:10.1071/WF08187.

Freeman, D.J., and Cattell, F.C.R., 1990, Woodburning as a source of atmospheric polycyclic aromatic hydrocarbons: Environmental Science & Technology, v. 24, p. 1581–1585, doi:10.1021/es00080a019.

Geptner, A.R., Alekseeva, T.A., and Pikovskii, Y.I., 2002, Polycyclic aromatic hydrocarbons in Holocene sediments and tephra of Iceland (composition and distribution features): Lithology and Mineral Resources, v. 37, p. 148–156, doi:10.1023/A:1014824517020.

Glasspool, I.J., and Scott, A.C., 2013, Identifying past fire events, *in* Belcher, C.M., ed., Fire phenomena and the Earth system: An interdisciplinary guide to fire science: Oxford, John Wiley & Sons, p. 179–205, doi:10.1002/9781118529539.ch10.

Glasspool, I.J., Scott, A.C., Waltham, D., Pronina, N., and Shao, L.Y., 2015, The impact of fire on the late Paleozoic Earth system: Frontiers in Plant Science, v. 6, p. 1–13, doi:10.3389/fpls.2015.00756.

Grasby, S.E., Sanei, H., and Beauchamp, B., 2011, Catastrophic dispersion of coal fly ash into oceans during the latest Permian extinction: Nature Geoscience, v. 4, p. 104–107, doi:10.1038/ngeo1069.

Han, D.X., and Yang, Q., 1980, Coal geology (third edition): Beijing, Coal Industry Publishing, 350 p. (in Chinese).

Hower, J.C., Misz-Keenan, M., O'Keefe, J.M.K., Mastalerz, M., Eble, C.F., Garrison, T.M., Johnston, M.N., and Stucker, J.D., 2013, Macrinite forms in Pennsylvanian coals: International Journal of Coal Geology, v. 116–117, p. 172–181, doi:10.1016/j.coal.2013.07.017.

Hudspith, V., Scott, A.C., Collinson, M.E., Pronina, N., and Beeley, T., 2012, Evaluating the extent to which wildfire history can be interpreted from inertinite distribution in coal pillars: An example from the Late Permian, Kuznetsk Basin, Russia: International Journal of Coal Geology, v. 89, p. 13–25, doi:10.1016/j.coal.2011.07.009.

International Committee for Coal and Organic Petrology, 2001, The new inertinite classification (ICCP System 1994): Fuel, v. 80, p. 459–471, doi:10.1016/S0016-2361(00)00102-2.

Isozaki, Y., 2009, Illawarra reversal: The fingerprint of a superplume that triggered Pangean breakup and the end-Guadalupian (Permian) mass extinction: Gondwana Research, v. 15, p. 421–432, doi:10.1016/j.gr.2008.12.007.

Jasper, A., Uhl, D., Guerra-Sommer, M., Bernardes-de-Oliveira, M.E.C., and Machado, N.T.G., 2011, Upper Paleozoic charcoal remains from South America: Multiple evidences of fire events in the coal bearing strata of the Paraná Basin, Brazil: Palaeogeography, Palaeoclimatology, Palaeoecology, v. 306, p. 205–218, doi:10.1016/j.palaeo.2011.04.022.

Jasper, A., Guerra-Sommer, M., Hamad, A.M.B.A., Bamford, M., Bernardes-de-Oliveira, M.E.C., Tewari, R., and Uhl, D., 2013, The burning of Gondwana: Permian fires on the southern continent—A palaeobotanical approach: Gondwana Research, v. 24, p. 148–160, doi:10.1016/j.gr.2012.08.017.

Jasper, A., Agnihotri, D., Tewari, R., Spiekermann, R., Pires, E.F., Da Rosa, Á.A.S., and Uhl, D., 2016a, Fires in the mire: Repeated fire events in Early Permian 'peat forming' vegetation of India: Geological Journal, doi:10.1002/gj.2860.

Jasper, A., Uhl, D., Agnihotri, D., Tewari, R., Pandita, S.K., Benicio, J.R.W., Pires, E.F., Da Rosa, Á.A.S., Bhat, G.D., and Pillai, S.S.K., 2016b, Evidence of wildfires in the Late Permian (Changsinghian) Zewan Formation of Kashmir, India: Current Science, v. 110, p. 419–423, doi:10.18520/cs/v110/i3/419-423.

Kauffmann, M., Jasper, A., Uhl, D., Meneghini, J., Osterkamp, I.C., Zvirtes, G., and Pires, E.F., 2016, Evidence for palaeo-wildfire in the Late Permian palaeotropics—Charcoal from the Motuca Formation in the Parnaíba Basin, Brazil: Palaeogeography, Palaeoclimatology, Palaeoecology, v. 450, p. 122–128, doi:10.1016/j.palaeo.2016.03.005.

Kwiecińska, B.K., and Petersen, H.I., 2004, Graphite, semi-graphite, natural coke and natural char classification ICCP system: International Journal of Coal Geology, v. 57, p. 99–116, doi:10.1016/j.coal.2003.09.003.

Kwiecińska, B.K., Hamburg, G., and Vleeskens, J.M., 1992, Formation temperature of natural coke in the Silesian coal basin, Poland. Evidence from pyrite and clays by SEM-EDX: International Journal of Coal Geology, v. 21, p. 217–235, doi:10.1016/0166-5162(92)90025-R.

Lenton, T.M., 2013, Fire feedbacks on atmospheric oxygen, *in* Belcher, C.M., eds., Fire phenomena and the Earth system: An interdisciplinary guide to fire science: Oxford, John Wiley & Sons, p. 289–308, doi:10.1002/9781118529539.ch15.

Li, H.Y., He, B., Xu, Y.G., and Huang, X.L., 2010, U-Pb and Hf isotope analyses of detrital zircons from late Paleozoic sediments: Insights into interactions of the North China Craton with surrounding plates: Journal of Asian Earth Sciences, v. 39, p. 335–346, doi:10.1016/j.jseaes.2010.05.002.

Li, J.Y., 2006, Permian geodynamic setting of northeast China and adjacent regions: Closure of the Paleo-Asian Ocean and subduction of the Paleo-Pacific plate: Journal of Asian Earth Sciences, v. 26, p. 207–224, doi:10.1016/j.jseaes.2005.09.001.

Liu, Y.S., Gao, S., Hu, Z.C., Gao, C.G., Zong, K.Q., and Wang, D.B., 2010, Continental and oceanic crust recycling-induced melt-peridotite interactions in the trans-North China orogen: U-Pb dating, Hf isotopes and trace elements in zircons from mantle xenoliths: Journal of Petrology, v. 51, p. 537–571, doi:10.1093/petrology/egp082.

Manfroi, J., Uhl, D., Guerra-Sommer, M., Francischini, H., Martinelli, A.G., Soares, M.B., and Jasper, A., 2015, Extending the database of Permian palaeo-wildfire on Gondwana: Charcoal remains from the Rio do Rasto Formation (Paraná Basin), Middle Permian, Rio Grande do Sul State, Brazil: Palaeogeography, Palaeoclimatology, Palaeoecology, v. 436, p. 77–84, doi:10.1016/j.palaeo.2015.07.003.

National Committee of Stratigraphy of China, 2014, The geologic time scale of China: Beijing, Geology Press, 1 p.

Noll, R., Uhl, D., and Lausberg, S., 2003, Brandstrukturen an Kieselhölzern der Donnersberg Formation (Oberes Rotliegend, Unterperm) des Saar-Nahe-Beckens (SW-Deutschland): Veröffentlichungen des Museums für Naturkunde Chemnitz, v. 26, p. 63–72.

Norin, E., 1922, The late Palaeozoic and early Mesozoic sediments of central Shansi: Geological Survey of China Bulletin, v. 4, p. 1–79.

Pyne, S.J., Andrews, P.L., and Laven, R.D., 1996, Introduction to wildland fire: New York, Wiley, p. 46–127.

Richards, A., Argles, T., Harris, N., Parrish, R., Ahmad, T., Darbyshire, F., and Draganits, E., 2005, Himalayan architecture constrained by isotopic tracers from clastic sediments: Earth and Planetary Science Letters, v. 236, p. 773–796, doi:10.1016/j.epsl.2005.05.034.

Rimmer, S.M., Hawkins, S.J., Scott, A.C., and Cressler, W.L., III, 2015, The rise of fire fossil: Fossil charcoal in late Devonian marine shales as an indicator of expanding terrestrial ecosystems, fire, and atmospheric change: American Journal of Science, v. 315, p. 713–733, doi:10.2475/08.2015.01.

Robson, B.E., Collinson, M.E., Riegel, W., Wilde, V., Scott, A.C., and Pancost, R.D., 2015, Early Paleogene wildfires in peat-forming environments at Schöningen, Germany: Palaeogeography, Palaeoclimatology, Palaeoecology, v. 437, p. 53–62, doi:10.1016/j.palaeo.2015.07.016.

Scott, A.C., 2010, Charcoal recognition, taphonomy and uses in palaeoenvironmental analysis: Palaeogeography, Palaeoclimatology, Palaeoecology, v. 291, p. 11–39, doi:10.1016/j.palaeo.2009.12.012.

Scott, A.C., and Glasspool, I.J., 2006, The diversification of Paleozoic fire systems and fluctuations in atmospheric oxygen concentration: National Academy of Sciences Proceedings, v. 103, p. 10861–10865, doi:10.1073/pnas.0604090103.

Scott, A.C., and Glasspool, I.J., 2007, Observations and experiments on the formation and origin of inertinite group macerals: International Journal of Coal Geology, v. 70, p. 53–66, doi:10.1016/j.coal.2006.02.009.

Scott, A.C., Chaloner, W.G., Belcher, C.M., and Roos, C., 2016, The interaction of fire and mankind: Introduction: Royal Society of London Philosophical Transactions, ser. B, v. 371, p. 1–8, doi:10.1098/rstb.2015.0162.

Shen, W.J., Sun, Y.G., Lin, Y.T., Liu, D.H., and Chai, P.X., 2011, Evidence for wildfire in the Meishan section and implications for Permian Triassic events: Geochimica et Cosmochimica Acta, v. 75, p. 1992–2006, doi:10.1016/j.gca.2011.01.027.

Shi, G.R., and Waterhouse, J.B., 2010, Late Palaeozoic global changes affecting high-latitude environments and biotas: An introduction: Palaeogeography, Palaeoclimatology, Palaeoecology, v. 298, p. 1–16, doi:10.1016/j.palaeo.2010.07.021.

Singh, M.P., and Shukla, R.R., 2004, Petrographic characteristics and depositional conditions of Permian coals of Pench, Kanhan, and Tawa Vally coalfields of Satpura Basin, Madhya Pradesh, India: International Journal of Coal Geology, v. 59, p. 209–243, doi:10.1016/j.coal.2004.02.002.

Stevens, L.G., Hilton, J., Bond, D.P.G., Glasspool, I., and Jardine, P.E., 2011, Radiation and extinction patterns in Permian floras from North China as indicators for environmental and climate change: Journal of the Geological Society [London], v. 168, p. 607–619, doi:10.1144/0016-76492010-042.

Sun, B.L., Zeng, F.G., Liu, C., Cui, X.Q., and Wang, W., 2014, Constraints on U-Pb dating of detrital zircon of the maximum depositional age for upper Paleozoic coal-bearing strata in Shanxi, Taiyuan and its stratigraphic significance: Acta Geologica Sinica, v. 88, p. 185–197.

Sun, Y.Z., Püttmann, W., Kalkreuth, W., and Horsfield, B., 2002, Petrologic and geochemical characteristics of seam 9–3 and Seam 2, Xingtai Coalfield, northern China: International Journal of Coal Geology, v. 49, p. 251–262, doi:10.1016/S0166-5162(01)00067-2.

Sýkorová, I., Pickel, W., Christanis, K., Wolf, M., Taylor, G.H., and Flores, D., 2005, Classification of huminite—ICCP System 1994: International Journal of Coal Geology, v. 62, p. 85–106, doi:10.1016/j.coal.2004.06.006.

Tanner, L.H., and Lucas, S.G., 2016, Stratigraphic distribution and significance of a 15 million-year record of fusain in the Upper Triassic Chinle Group, southwestern USA: Palaeogeography, Palaeoclimatology, Palaeoecology, 461, p.261–271, doi:10.1016/j.palaeo.2016.08.034.

Thomas, B.M., et al., 2004, Unique marine Permian-Triassic boundary section from Western Australia: Australian Journal of Earth Sciences, v. 51, p. 423–430, doi:10.1111/j.1400-0952.2004.01066.x.

Uhl, D., and Kerp, H., 2003, Wildfires in the late Palaeozoic of Central Europe—The Zechstein (Upper Permian) of NW-Hesse (Germany): Palaeogeography, Palaeoclimatology, Palaeoecology, v. 199, p. 1–15, doi:10.1016/S0031-0182(03)00482-6.

Uhl, D., Lausberg, S., Noll, R., and Stapf, K.R.G., 2004, Wildfires in the late Palaeozoic of central Europe—An overview of the Rotliegend (Upper Carboniferous–Lower Permian) of the Saar-Nahe Basin (SW-Germany): Palaeogeography, Palaeoclimatology, Palaeoecology, v. 207, p. 23–35, doi:10.1016/j.palaeo.2004.01.019.

Uhl, D., Jasper, A., Hamad, A.M.B., and Montenari, M., 2008, Permian and Triassic wildfires and atmospheric oxygen levels: Proceedings, 1st WSEAS International Conference on Environmental and Geological Science and Engineering: World Scientific and Engineering Academy and Society, p. 179–187.

Uhl, D., Butzmann, R., Fischer, T.C., Meller, B., and Kustatscher, E., 2012, Wildfires in the late Palaeozoic and Mesozoic of the Southern Alps—The late Permian of the Bletterbach-Butterloch area (northern Italy): Rivista Italiana di Paleontologia e Stratigrafia, v. 118, p. 223–233, doi:10.13130/2039-4942/6002.

van de Schootbrugge, B.V., et al., 2009, Floral changes across the Triassic/Jurassic boundary linked to flood basalt volcanism: Nature Geoscience, v. 2, p. 589–594, doi:10.1038/ngeo577.

Veevers, J.J., Saeed, A., Belousova, E.A., and Griffin, W.L., 2005, U-Pb ages and source composition by Hf-isotope and trace-element analysis of detrital zircons in Permian sandstone and modern sand from southwestern Australia and a review of the paleogeographical and denudational history of the Yilgarn Craton: Earth-Science Reviews, v. 68, p. 245–279, doi:10.1016/j.earscirev.2004.05.005.

Walker, J.D., and Geissman, J.W., compilers, 2009, Geologic time scale: Boulder, Colorado, Geological Society of America, doi:10.1130/2009.CTS004R2C.

Wan, T.F., and Zeng, H.L., 2002, The distinctive characteristics of the Sino-Korean and the Yangtze plates: Journal of Asian Earth Sciences, v. 20, p. 881–888, doi:10.1016/S1367-9120(01)00068-2.

Wang, H.Z., Chu, X.C., Liu, B.P., Hou, H.F., and Ma, L.F., 1985, Atlas of the palaeogeography of China: Beijing, Cartographic Press, 143 p. (in Chinese with English abstract).

Wang, J., 2010, Late Paleozoic macrofloral assemblages from Weibei Coalfield, with reference to vegetational change through the late Paleozoic ice-age in the North China block: International Journal of Coal Geology, v. 83, p. 292–317, doi:10.1016/j.coal.2009.10.007.

Wang, J., and Pfefferkorn, H.W., 2013, The Carboniferous-Permian transition on the North China microcontinent—Ocean climate in the tropics: International Journal of Coal Geology, v. 119, p. 106–113, doi:10.1016/j.coal.2013.07.022.

Wang, Z.-Q., and Chen, A.-S., 2001, Traces of arborescent lycopsids and dieback of the forest vegetation in relation to the terminal Permian mass extinction in North China: Review of Palaeobotany and Palynology, v. 117, p. 217–243, doi:10.1016/S0034-6667(01)00094-X.

Wignall, P.B., et al., 2009, Volcanism, mass extinction, and carbon isotope fluctuations in the Middle Permian of China: Science, v. 324, p. 1179–1182, doi:10.1126/science.1171956.

Wildman, R.A., Hickey, L.J., Dickinson, M.B., Berner, R.A., Robinson, J.M., Dietrich, M., Essenhigh, R.H., and Wildman, C.B., 2004, Burning of forest materials under late Paleozoic high atmospheric oxygen levels: Geology, v. 32, p. 457–460, doi:10.1130/G20255.1.

Xie, S.C., Pancost, R.D., Huang, J.H., Wignall, P.B., Yu, J.X., Tang, X.Y., Chen, L., Huang, X.Y., and Lai, X.L., 2007, Changes in the global carbon cycle occurred as two episodes during the Permian–Triassic crisis: Geology, v. 35, p. 1083–1086, doi:10.1130/G24224A.1.

Yan, M.X., Wan, M.L., He, X.Z., Hou, X.D., and Wang, J., 2016, First report of Cisuralian (early Permian) charcoal layers within a coal bed from Baode, North China with reference to global wildfire distribution: Palaeogeography, Palaeoclimatology, Palaeoecology, v. 459, p. 394–408, doi:10.1016/j.palaeo.2016.07.031.

Yang, J.H., Wu, F.Y., Shao, J.A., Wilde, S.A., Xie, L.W., and Liu, X.M., 2006, Constraints on the timing of uplift of the Yanshan fold and thrust belt, North China: Earth and Planetary Science Letters, v. 246, p. 336–352, doi:10.1016/j.epsl.2006.04.029.

Zhang, K.J., 1997, North and South China collision along the eastern and southern North China margins: Tectonophysics, v. 270, p. 145–156, doi:10.1016/S0040-1951(96)00208-9.

Zhao, G.C., Cao, L., Wilde, S., Sun, M., Choe, W.J., and Li, S.Z., 2006, Implications based on the first SHRIMP U-Pb zircon dating on Precambrian granitoid rocks in North Korea: Earth and Planetary Science Letters, v. 251, p. 365–379, doi:10.1016/j.epsl.2006.09.021.

Zhao, Y., Chen, B., Zhang, S.H., Liu, J.M., Hu, J.M., Liu, J., and Pei, J.L., 2010, Pre-Yanshanian geological events in the northern margin of the North China Craton and its adjacent areas: Geology in China, v. 37, p. 900–915 (in Chinese with English abstract).

Zhong, N.N., and Smyth, M., 1997, Striking liptinitic bark remains peculiar to some Late Permian Chinese coals: International Journal of Coal Geology, v. 33, p. 333–349, doi:10.1016/S0166-5162(96)00050-X.

Zhou, G.Q., Jiang, Y.F., Gao, F., and Xu, X.Q., 2015, The features of petrology and quality of coal in Late Triassic No. 5 coal in Zichang mining area in Shaanxi Province: Chinese Coal, v. 41, p. 30–34 (in Chinese with English abstract).

MANUSCRIPT RECEIVED 20 DECEMBER 2016
REVISED MANUSCRIPT RECEIVED 17 MARCH 2017
MANUSCRIPT ACCEPTED 18 APRIL 2017

Printed in the USA